15

Numerical Prediction of Fire Whirlwind Outbreak and Scale Effect of Whirlwind Behavior

Seigo Sakai
Yokohama National University
Japan

1. Introduction

Our Japanese, especially the residents in east area of Japan, have experienced a large earthquake on March 11, 2011, i.e. East Japan great earthquake disaster (Takewaki et al., 2011). There were a lot of fires in the northeast area of Japan, for example in Kesen-numa City. Despite of a number of town area fires, a fire whirlwind was never observed in this disaster. However, fire whirlwind is still one of the concerned accidents in the earthquake (Hough & Bilham; 2005).

When a large-scale wide area fire such as a town area fire or a forest fire occurs, there can be a strong rotating flow to be called fire whirlwind. A fire whirlwind is a tornado that includes flames, hot winds and sparks. The fire whirlwind is regarded as the worst case which we should avoid at the time of a large-scale fire, because the whirlwind itself is critical and scatters sparks widely to promote spread of a fire.

As a fire occurs, a flame makes an ascending current of air and uses up neighboring oxygen. Furthermore, to collect oxygen from a wide area, there is a current of air against the flame, resulting in big natural convection in the fire current of air. When the wind from a certain specified direction blows in this fire current of air, homogeneity of suction of air with an ascending current of air collapses. Then, a vortex is easy to come to occur, the fire current of air becomes a fire whirlwind that is an ascending current of air accompanied with rotating. Fire whirlwind may be pushed away by wind downstream, or may move in search of oxygen.

Aiming at a property and elucidation of an outbreak factor of fire whirlwind as examples of the pasts for a lesson, investigation and a reproduction experiment of the outbreak situation (Graham, 1955; Emmons & Ying, 1967; Byram & Martin, 1970; Haines & Updike, 1971; Martin et al., 1976; Muraszew et al., 1979; Emori & Saito, 1982; Satoh & Yang, 1996; Hayashi et al., 2003; Liu, 2005; Kuwana et al., 2007; Liu et al., 2007; Kuwana et al., 2008; Chuah et al., 2011), numerical analysis are performed till now (Satoh & Yang, 1997; Battaglia et al., 2000a; Battaglia et al., 2000b; Snegirev et al., 2004; Hassan et al., 2005; Chuah et al., 2007; Grishin, 2007; Grishin et al., 2009). Though various factors are thought about outbreak of a fire whirlwind, such as climatic condition or existence of underground flammable gas, it is hard

to say that property and outbreak mechanism of a fire whirlwind are to be elucidated enough.

Therefore, in this study, it is firstly aimed to get basic knowledge to elucidate outbreak mechanism of fire whirlwind and the property, by evaluating influence between a natural convection generated by the fire and the wind blowing to fire whirlwind on the ground utilizing numerical analysis. It is secondly examined whether a relationship exists between a real phenomenon and the phenomenon in reduction models, performing the numerical analysis of a fire whirlwind with respect to scale effect.

Three dimensional analyses are performed to investigate the thermal and flow fields by using an analytical software FLUENT 6.3. Natural convection is caused from a plane source of constant heat flux or constant temperature in the flat ground large enough. It is observed and evaluated whether a fire whirlwind occurs or not in a constant wind of air. It is also observed and evaluated how the whirlwind behaves in case that the whirlwind occurs. Then, it is analyzed that those swirling flow in original scale, 1/10 scale, 1/50 scale, 1/100 scale from the original brake out to vanish. As an analytical condition, parameter calculation is repeated to get the velocity of a parallel flow which is the easiest to occur the swirling flow for each reduction model, and then scale effect is discussed by comparing the velocity of the natural convection, the velocity of the parallel flow, the center pressure of the whirlwind and the continuance time of the swirling flow. For making of analysis models, a representative example of the fire whirlwind that occurred at Tokyo in the Great Kanto Earthquake (1923) is referred, and three types of heat source model (L-character model, random model and C-character model) are constructed.

2. Nomenclature

a	Absorption coefficient of air
$C_{1\varepsilon}, C_{2\varepsilon}, C_{3\varepsilon}$	Constants for standard k-ε turbulent model
$c_{p.j}$	Specific heat of species of j at constant pressure
E	Energy
$\vec{F}$	External force vector
G	Irradiance
G_b	Turbulent kinetic energy production due to buoyancy force
G_k	Turbulent kinetic energy production due to gradient of time-averaged velocity
$\vec{g}$	Gravitational acceleration vector
h	Sensible heat enthalpy
h_j	Sensible heat enthalpy of chemical species j
I	Unit tensor
$\vec{J}_j$	Diffusive flux vector of chemical species j
k	Turbulent kinetic energy
k_{eff}	Effective thermal conductivity
p	Pressure

q_r	Radiative heat flux
S_h	Heat source including volumetric heat generation
S_k ,S_ε	Source terms for k and ε
T	Temperature
T_{ref}	Reference temperature
t	Time
$\vec{v}$	Velocity vector
Y_j	Mass fraction of chemical species j
Y_M	Expansion dissipation term for k

Greek symbols

ε	Turbulent energy dissipation rate
μ	Viscosity of air
μ_t	Turbulent viscosity of air
ρ	Density of air
σ	Stefan-Boltzmann constant
σ_k ,σ_ε	Turbulent Prandtl numbers for k and ε
$\overline{\overline{\tau}}$	Shear stress tensor
$\overline{\overline{\tau}}_{eff}$	Effective shear stress

3. Governing equations

In this analysis, chemical reaction and combustion phenomenon are not dealt with, and driving force for convective heat transfer is due to density change of air from the heat source. Therefore, governing equations of the phenomenon are as follows (Fluent Inc/Flient Asia Pacific, 2006).

Mass conservation equation

$$\frac{\partial \rho}{\partial t} + \nabla \cdot (\rho \vec{v}) = 0 \,. \tag{1}$$

Navier-Stokes equation

$$\frac{\partial}{\partial t}(\rho \vec{v}) + \nabla \cdot (\rho \vec{v} \vec{v}) = -\nabla p + \nabla \cdot \left(\overline{\overline{\tau}}\right) + \rho \vec{g} + \vec{F} \,, \tag{2}$$

where

$$\overline{\overline{\tau}} = \mu \left[(\nabla \vec{v} + \nabla \vec{v}^T) - \frac{2}{3} \nabla \cdot \vec{v} I \right], \tag{3}$$

and the second term of right side shows effect of volume expansion.

Energy equation

$$\frac{\partial}{\partial t}(\rho E) + \nabla \cdot \{\vec{v}(\rho E + p)\} = \nabla \cdot \left\{ k_{eff} \nabla T - \sum h_j \vec{J}_j + \left(\bar{\bar{\tau}}_{eff} \cdot \vec{v} \right) \right\} + S_h \,. \tag{4}$$

The first, second and third term of right side show energy transfers by conduction, diffusion of chemical species, and viscous dissipation, respectively. In equation (4),

$$E = h - \frac{p}{\rho} + \frac{v^2}{2}, \tag{5}$$

and given for ideal gas as

$$h = \sum_j Y_j h_j \,. \tag{6}$$

h_j is given as follows.

$$h_j = \int_{T_{ref}}^{T} c_{p,j} dT \,. \tag{7}$$

where T_{ref} is set to 300K in this analysis.

Equation of Turbulent model

Turbulent flow is treated in the analysis, and the standard *k-ε* model is employed.

$$\frac{\partial}{\partial t}(\rho k) + \frac{\partial}{\partial x_i}(\rho k u_i) = \frac{\partial}{\partial x_j}\left[\left(\mu + \frac{\mu_t}{\sigma_k} \right) \frac{\partial k}{\partial x_j} \right] + G_k + G_b - \rho\varepsilon - Y_M + S_k \,, \tag{8}$$

$$\frac{\partial}{\partial t}(\rho \varepsilon) + \frac{\partial}{\partial x_i}(\rho \varepsilon u_i) = \frac{\partial}{\partial x_j}\left[\left(\mu + \frac{\mu_t}{\sigma_\varepsilon} \right) \frac{\partial \varepsilon}{\partial x_j} \right] + C_{l\varepsilon} \frac{\varepsilon}{k}(G_k + C_{3\varepsilon} G_b) - C_{2\varepsilon} \rho \frac{\varepsilon^2}{k} + S_\varepsilon \,. \tag{9}$$

Radiation model

P-1 radiative heat exchange model (Siegel & Howell, 2002) is also employed to simulate the radiative heat transfer from the heat source at high temperature. The equation of P-1 model is as follows.

$$-\nabla q_r = aG - 4a\sigma T^4 \,. \tag{10}$$

Numerical analysis is performed three-dimensionally with FLUENT6.3.

4. Analysis model

A calculation domain is taken enough widely to avoid the influence of natural convection due to heat source. Depth and width are 2000m and height is 500m. Heat source is modeled by a combination of 16 squares (200m×200m) at the center of bottom in the domain. Each square is given a constant value of heat flux individually, and various profiles of large-scale fires are easily constructed. While heat flux of house fire is about 1.0 MW/m², simulation is performed at 0.03MW/m² of heat flux. Fig. 1 shows the calculation domain for analysis.

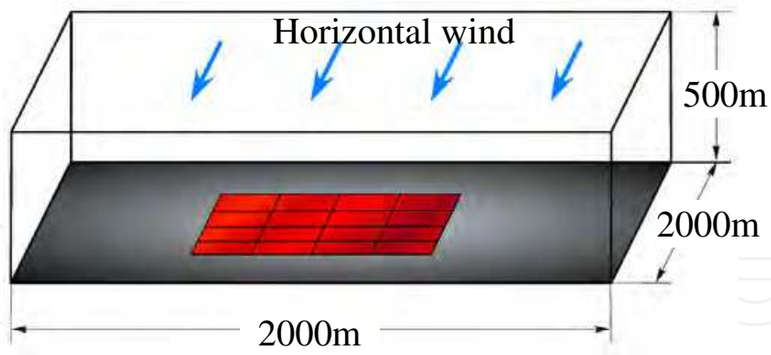

Fig. 1. Calculation domain for analysis

Three models are considered in the analysis. One is based on the large-scale fire at the Great Kanto Earthquake (1923 in Japan), and the profile of the heat source at the bottom is "L-character" type (Model 1). The second one is the profile in which the heat source is randomly dispersed at the bottom (Model 2). The third one is the profile of the heat source at the bottom is "C-character" type (Model 3). Fig. 2 shows the profiles of the heat source.

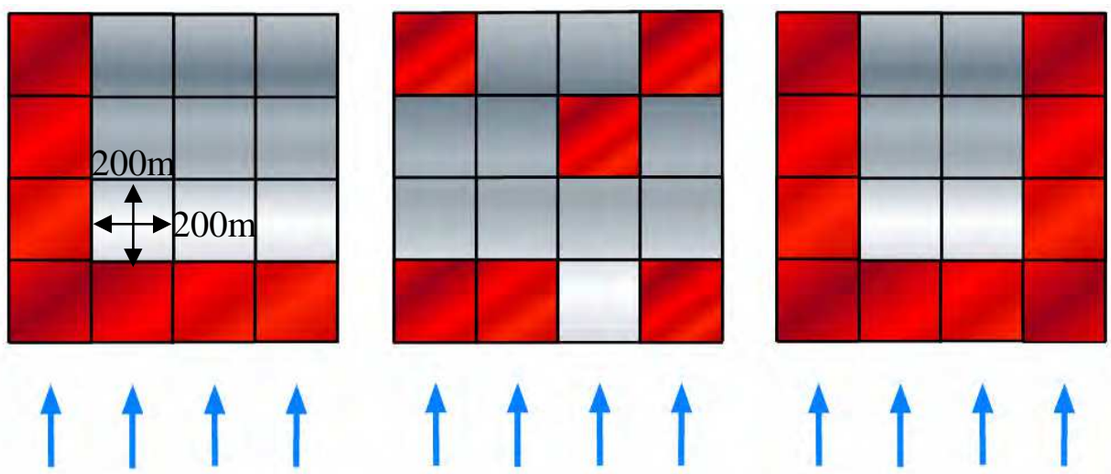

(a) L-character type (Model 1) (b) random type (Model 2) (c) C-character type (Model3)

Fig. 2. Profiles of heat source at the bottom

Initially, air is uniformly enclosed in the domain at atmospheric pressure and temperature of 300K. Bottom of the domain assumes adiabatic except 16 squares of modeled heat source. Four sides and top of the domain is free for inflow and outflow.

5. Results and discussions

5.1 Outbreak of fire whirlwind

In this section, it is aimed to get basic knowledge to elucidate outbreak mechanism of fire whirlwind and the property, by evaluating influence between a natural convection generated by the fire and the wind blowing to fire whirlwind on the ground utilizing numerical analysis (Sakai & Watanabe, 2007).

For 5 minutes from calculation start, natural convection is developed in the domain. Then, horizontal air flow is introduced from one side of the domain at 4, 6 and 8m/s of the velocity. Wind on the ground is modeled by the air flow. Calculation is continued for several minutes from the introduction of the air flow.

5.1.1 Model 1

Figs. 3 and 4 are the sample of streamline distribution after 5 minutes and that after 30 minutes for the wind of 4m/s. These streamlines are drawn from the pressure surface whose pressure is lower by 30 Pa from the atmospheric pressure, and are colored by velocity magnitude. Number of generated fire whirlwind and behavior of the whirlwind (movement and extinction) are altered dependent on the velocity of wind. It is summarized in the Fig. 5.

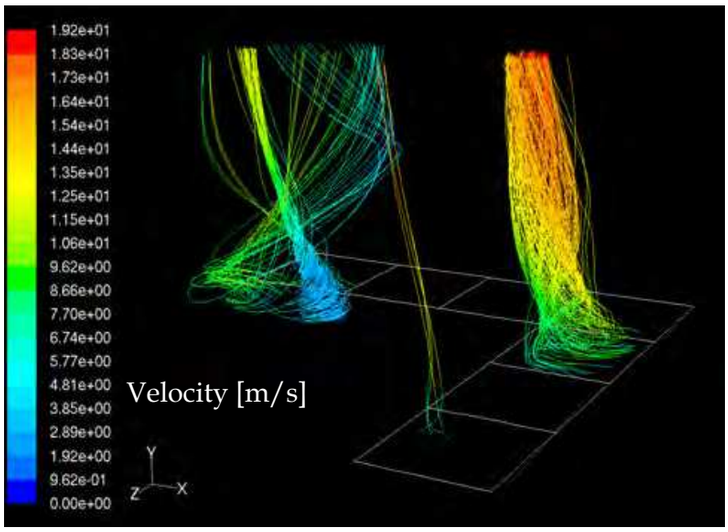

Fig. 3. Distribution of streamlines after 5 minutes for the wind of 4m/s

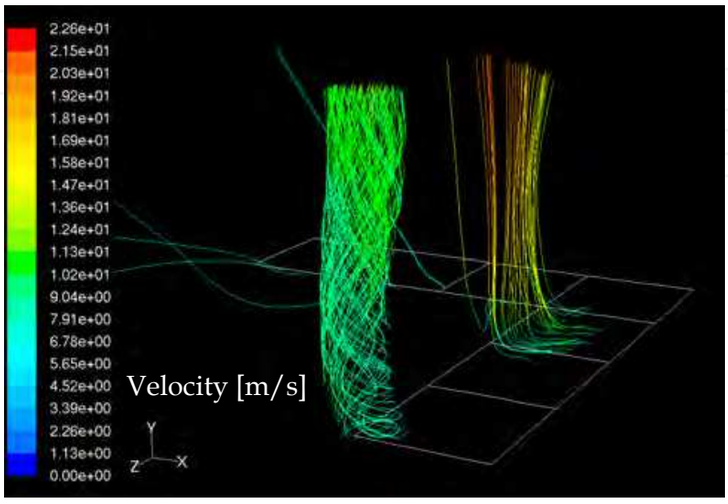

Fig. 4. Distribution of streamlines after 30 minutes for the wind of 4m/s

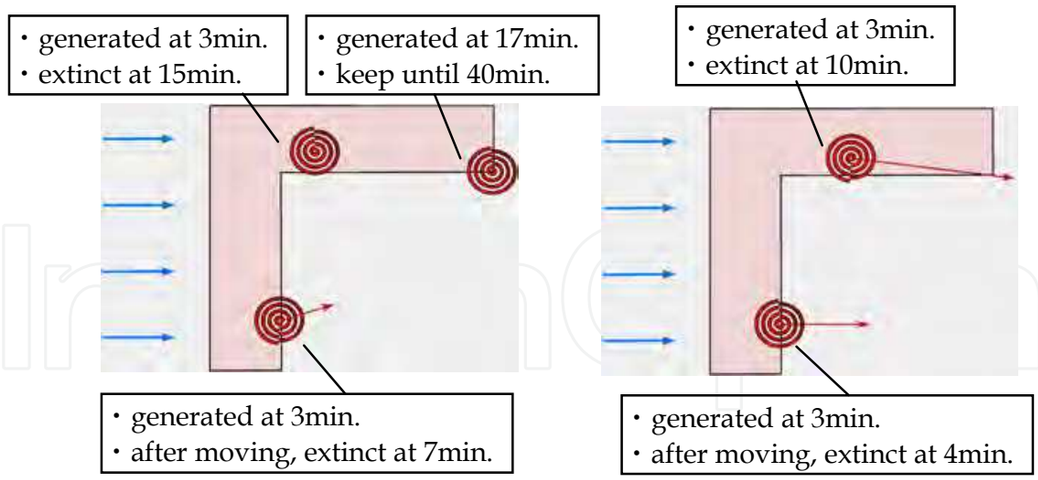

(a) wind of 4m/s (b) wind of 6m/s

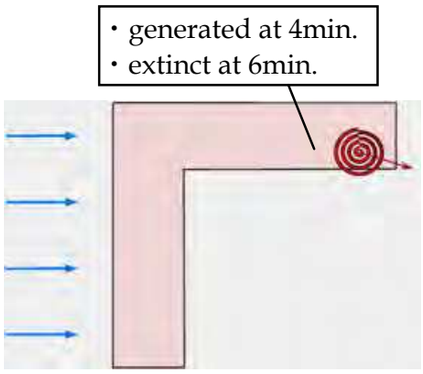

(c) wind of 8m/s

Fig. 5. Summary of generation and extinction of fire whirlwind in Model 1

Red arrows in the figure show the distance from the generation point for the duration time of the whirlwind. In the case of wind of 4m/s, three whirlwinds are generated, and duration time is longer than the other 2 cases. In the case of wind of 6m/s, two whirlwinds are generated, and duration time is shorter than the case of 4m/s. In the case of wind of 8m/s, just one whirlwind is generated, and duration time is the shortest in 3 cases.

Generation points of the whirlwind are located at the tips and corner of "L" character. Fig. 6 shows a numerical result of streamlines in natural convective heat transfer at 5 minutes (no wind). The points where the natural convective flow develops become origins of the fire whirlwind.

The number of the generated whirlwind is decreased as the velocity of wind is increased. This is because too fast wind blows the ascending current of air by natural convection to the downstream. Figs. 7 and 8 are side views of streamlines for the wind of 4m/s in Model 1. The former is streamlines after 18.6 minutes, and the latter is that after 26.6 minutes. As time passes, it is shown that the ascending current of air by natural convection is blown to the downstream by the wind.

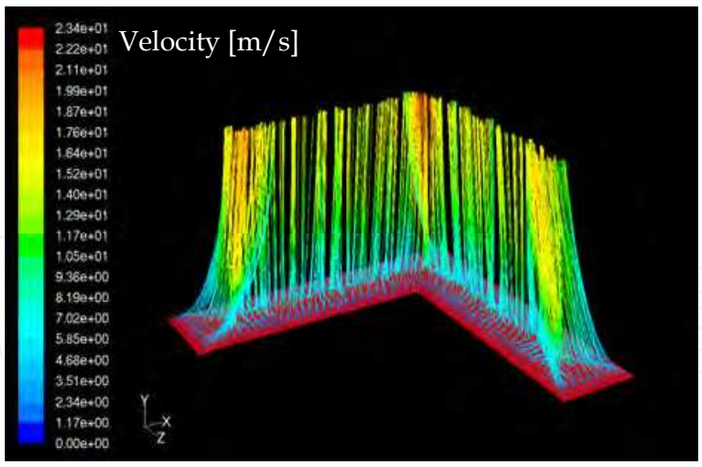

Fig. 6. Distribution of streamlines after 5 minutes in natural convective heat transfer

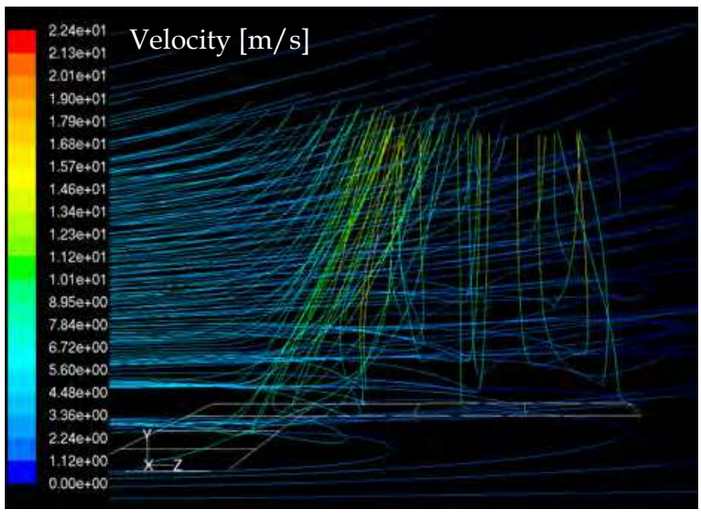

Fig. 7. Side view of streamlines after 18.6 minutes for the wind of 4m/s in Model 1

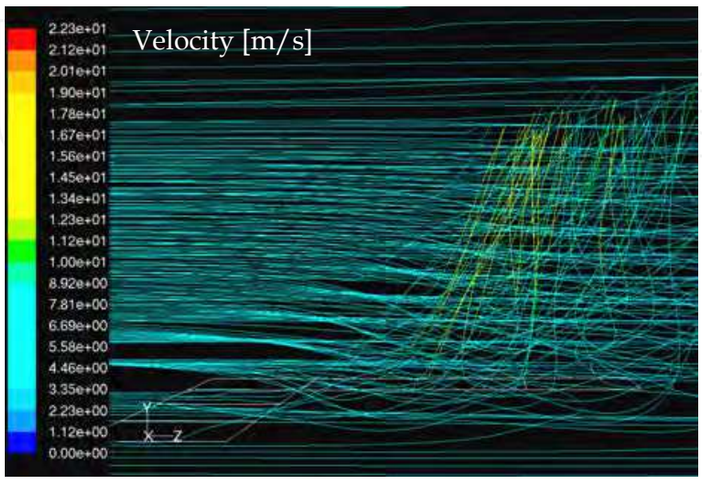

Fig. 8. Side view of streamlines after 26.6 minutes for the wind of 4m/s in Model 1

5.1.2 Model 2

Figs. 9 and 10 are the samples of streamline distribution after 15 minutes and that after 35 minutes for the wind of 4m/s. These streamlines are also drawn from the pressure surface whose pressure is lower by 30 Pa from the atmospheric pressure, and are colored by velocity magnitude.

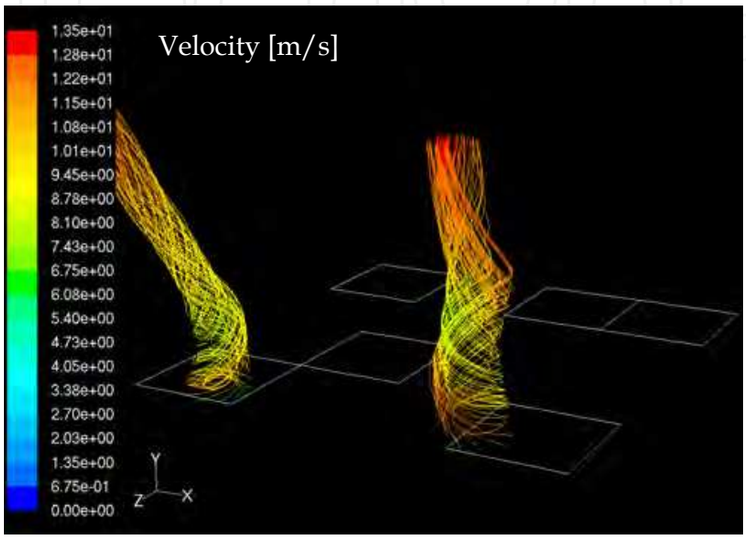

Fig. 9. Distribution of streamlines after 15 minutes for the wind of 4m/s

In contrast with the results in the "L" character type, number of generated fire whirlwind is almost the same, i.e. two, even if the velocity of wind is altered. Behavior of the whirlwind (movement and extinction) is also almost the same in the both cases of wind velocity 6 and 8m/s. In the case of wind velocity 4m/s, a whirlwind generated after 12 minutes around two heat sources surfaces moves and once weakened because it is apart from the heat source. Then, it is strengthened again as it returns on the heat source. The point that we should pay attention to is that two fire whirlwinds in the case of 4m/s (one is generated after 12 minutes and remains until the end of simulation, and the other is generated at 35 minutes and extinct at 39 minutes) move to the upstream.

Generation points of the whirlwind are located at the downstream heat source, and the number of the generated whirlwind is almost the same though the velocity of wind is varied. In the random type of heat source surfaces, there is a lack of heat source in the upstream. Therefore, interaction between the ascending current of air by natural convection and wind is disturbed (See Fig. 11). Then, the interacted flow arrives at the downstream heat source, and easily generates the fire whirlwind because heat is supplied.

It is summarized in the Fig. 12. Duration time of the whirlwind becomes shorter as the velocity of wind is increased.

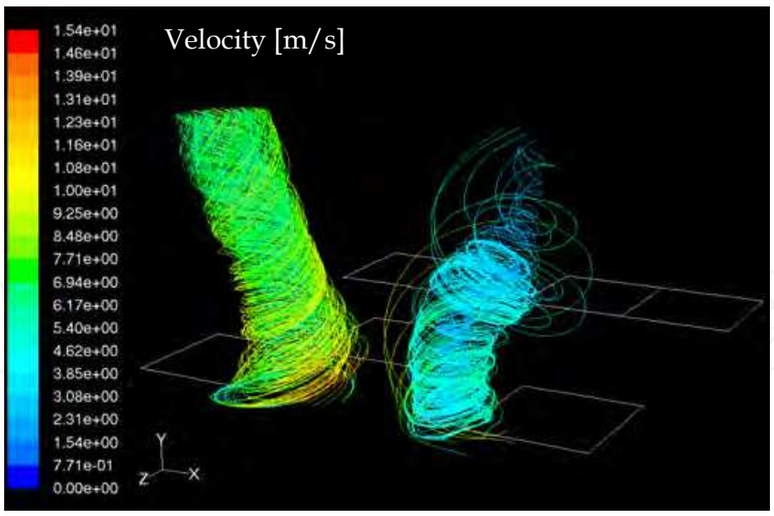

Fig. 10. Distribution of streamlines after 35 minutes for the wind of 4m/s

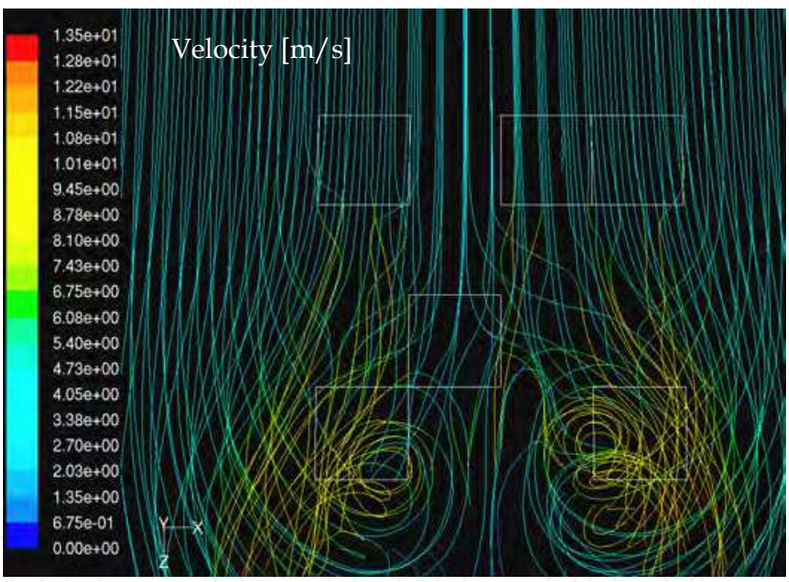

Fig. 11. Upper view of streamlines after 18 minutes for the wind of 4m/s in Model 2.

5.1.3 Summary

As a result of numerical analysis, interaction between the ascending current of air by natural convection and wind results in a fire whirlwind. The whirlwind sometimes moves and extinct. Generation points of the whirlwind are located at the tips and corner in the model of "L" character type. The points where the natural convective flow develops becomes origins of the fire whirlwind. Generation points of the whirlwind in the model of random type are located at the downstream heat source, and the number of the generated whirlwind is almost the same though the velocity of wind is varied. This is because the ascending current of air by natural convection is partially disturbed by the wind.

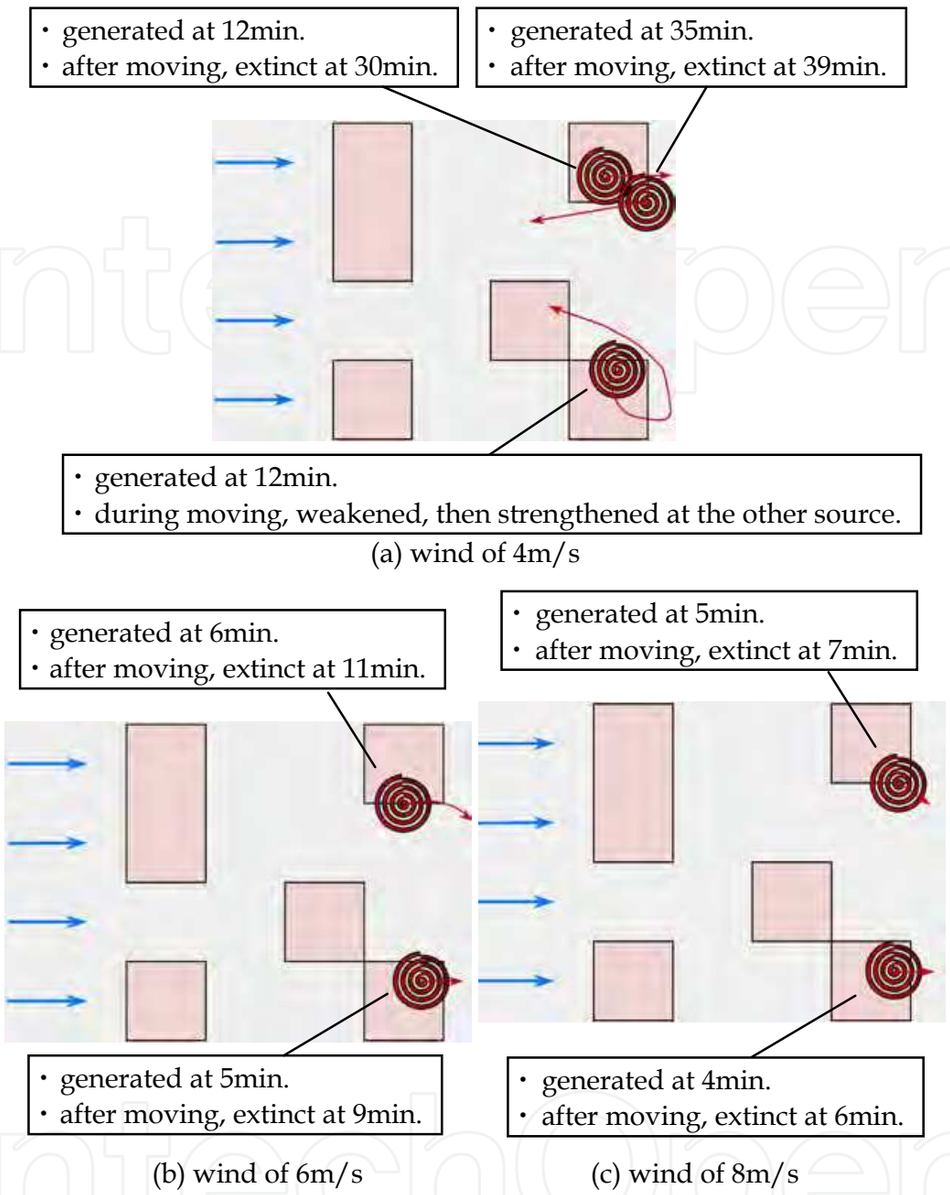

Fig. 12. Summary of generation and extinction of fire whirlwind in Model 2

5.2 Scale effect analysis

In this section, performing the numerical analysis of fire whirlwind with respect to scale effect, it is examined whether a relationship exists between a real phenomenon and the phenomenon in the reduction model with taking into account radiative heat transfer (Sakai & Miyagi, 2010).

Preceding the parametric calculation study, grid sensitivity for numerical result is evaluated. Residuals of continuity, velocity components, energy, turbulent energy and dissipation ratio of turbulent energy are derived and those absolute criteria are set to 10^{-3}

except 10^{-6} for energy to judge the convergence. For all scale ratios, grid number is altered and grid sensitivity is checked. Even if the coarse mesh number of 570700 cells and 1442164 faces is utilized for calculation, those residuals are well converged within 1000 iterations for each time step. Therefore, mesh number of 570700 cells and 1442164 faces is employed to attain the precision and calculation speed.

5.2.1 Effect of radiative heat exchange

In our previous study, radiative heat exchange was not considered to simulate the whirlwind, because we had to simplify the real phenomenon of the whirlwind into the fundamental thermal and flow fields as much as possible (Sakai and Watanabe, 2007). However, radiative heat exchange plays an important role in the heat transfer at the higher temperature field. Therefore, the P-1 model is utilized to simulate the radiative heat transfer from the heat source at high temperature.

Fig. 13 shows numerical results of streamlines in natural convective heat transfer at 5 minutes (no horizontal wind) for the L-character heat source in the original scale; (a) is the case of no radiative heat exchange considered, and (b) is the case of radiative heat exchange considered. Colors of streamlines show the temperature of the upward flow.

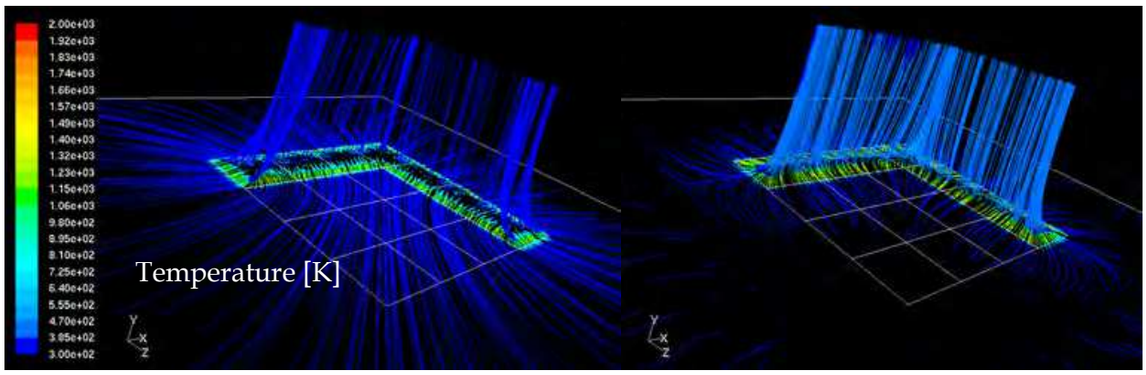

(a) No radiative heat exchange considered (b) Radiative heat exchange considered

Fig. 13. Distribution of streamlines after 5 minutes in natural convective heat transfer

In the case of no radiative heat exchange considered, temperature decreases within a few decade meters from the heat source. Therefore, air above the heat source plays an adiabatic role to prevent the heat transfer to the upper air layer. On the other hand, in the case of radiative exchange considered, heat from the heat source flows more to the upper air layer, resulting in more developed upward flow. In the case of no radiative exchange considered, the maximum upward velocity of natural convection and the appropriate velocity of horizontal wind to generate swirling flow are 23.5 m/s and 4 m/s, respectively. In the case of radiative exchange considered, the maximum upward velocity of natural convection and the appropriate velocity of horizontal wind are increased to 65.2 m/s and 11 m/s, respectively, due to the effective heat transfer. It is clarified that the radiative heat exchange must be considered to precisely simulate the fire whirlwind. The following numerical results are taking into account the radiative heat exchange.

5.2.2 Generation and extinction of swirling flow in Model 1

Fig. 14 shows samples of pressure field at the bottom surface and streamline distributions for the original scale simulation; (a) is at 2 minutes since the introduction of horizontal wind, (b) is at 5.5 minutes since the introduction of horizontal wind, and (c) is at 7.5 minutes since the introduction of horizontal wind. These streamlines are drawn from the bottom surface, and are colored by velocity magnitude.

From Fig. 14 (a), two whirlwinds are generated and generation points of the whirlwind are located at the tip and the corner of "L" character. At 5.5 minutes since the introduction of horizontal wind, a whirlwind generated at the tip is extinguished, and the other whirlwind is flown to the downstream (See Fig. 14 (b)). The remaining whirlwind is the strongest at this time, and the maximum center pressure of the whirlwind is lower than the atmospheric pressure by 1,061Pa. At 7.5 minutes since the introduction of horizontal wind, the remaining whirlwind is divided into two whirlwinds (See Fig. 14 (c)), and is going to be extinguished at 10 minutes since the introduction of horizontal wind.

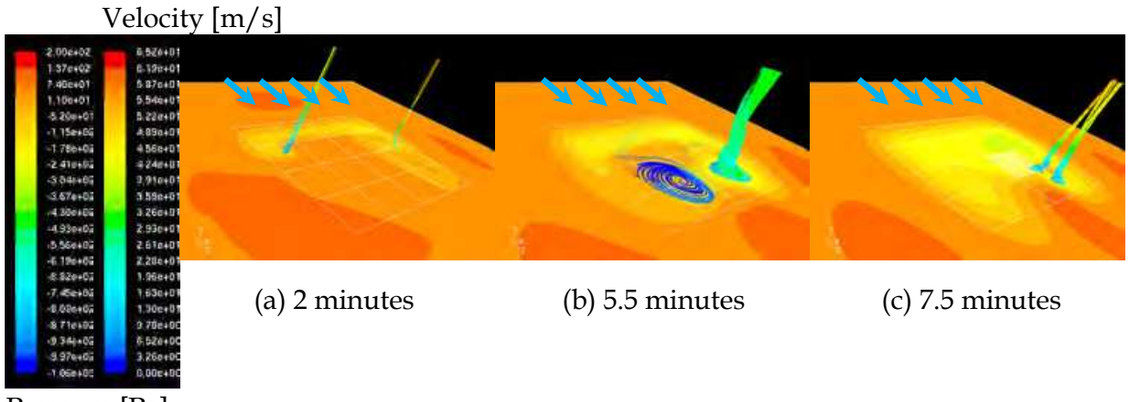

Fig. 14. Pressure field at the bottom surface and streamline distributions since the introduction of horizontal wind in Model 1

Numerical calculation is performed not only for the case of the original size, but also for 1/10 scale, 1/50 scale and 1/100 scale. In the original size calculation, natural convection is developed in the domain after 5 minutes. The smaller the scale is, the shorter the time necessary to develop the natural convection is. The times necessary to develop the natural convection are 90 seconds for 1/10 scale model, 45 seconds for 1/50 scale model, and 30 seconds for 1/100 scale model. This is because dynamics between the original size and scaled models are said to be similar if the rate of the scale ratio to the square of velocity (or time) are the same, in which Froude numbers are the same.

After defining the appropriate velocity of horizontal wind to generate swirling flow, behavior of the whirlwind (movement and extinction) is observed for all the cases. Number of generated fire whirlwind and behavior of the whirlwind are almost the same for all the cases. Therefore, characteristic physical quantities of whirlwind are discussed by comparing with scale ratio and square root of scale ratio in the followings.

5.2.2.1 Pressure of whirlwind

Fig. 15 shows relation among the scale ratio, the square root of scale ratio, and pressure at the bottom of natural convection after each period necessary to develop the natural convection. Taken the original size as a standard, the pressure at the bottom of natural convection is more coincident with the scale ratio rather than the square root of scale ratio.

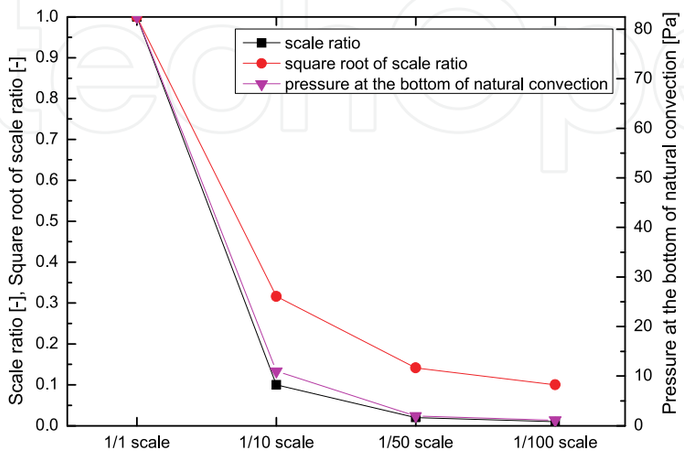

Fig. 15. Relation among scale ratio, square root of scale ratio, and pressure at the bottom of natural convection in Model 1

Fig. 16 shows relation among the scale ratio, the square root of scale ratio, and the maximum center pressure of whirlwind, which is lower than the atmospheric pressure. (The times of the strongest whirlwind generation after the introduction of the horizontal wind, i.e. the times when the center pressure of whirlwind is maximum, are different for all cases, and discussed in the next subsubsection.) The maximum center pressure of whirlwind is also more coincident with the scale ratio rather than the square root of scale ratio. Therefore, scale effect is recognized, in which pressure of whirlwind is coincident with the scale ratio.

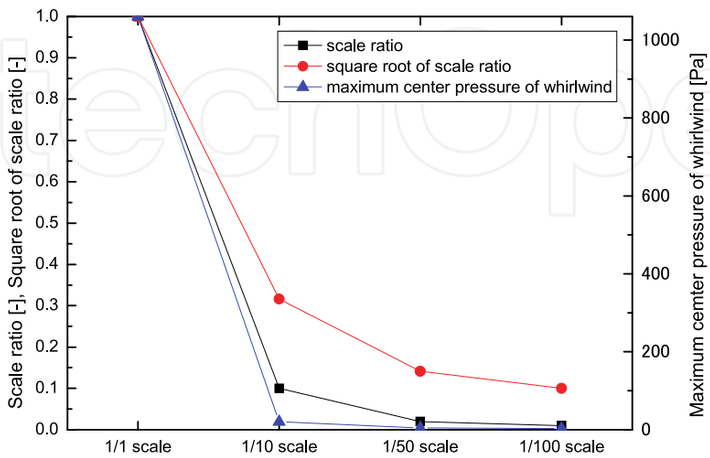

Fig. 16. Relation among scale ratio, square root of scale ratio, and maximum center pressure of whirlwind in Model 1

5.2.2.2 Time variation of whirlwind

Figs. 17 and 18 show relation among the scale ratio, the square root of scale ratio, and times of whirlwind generation and extinction since introduction of horizontal wind. Taken the original size as a standard, the times of whirlwind generation and extinction since introduction of horizontal wind are more coincident with the square root of scale ratio rather than the scale ratio. Duration time of whirlwind is derived from the times of whirlwind generation and extinction since introduction of horizontal wind. As a matter of course, the duration time is more coincident with the square root of scale ratio rather than the scale ratio.

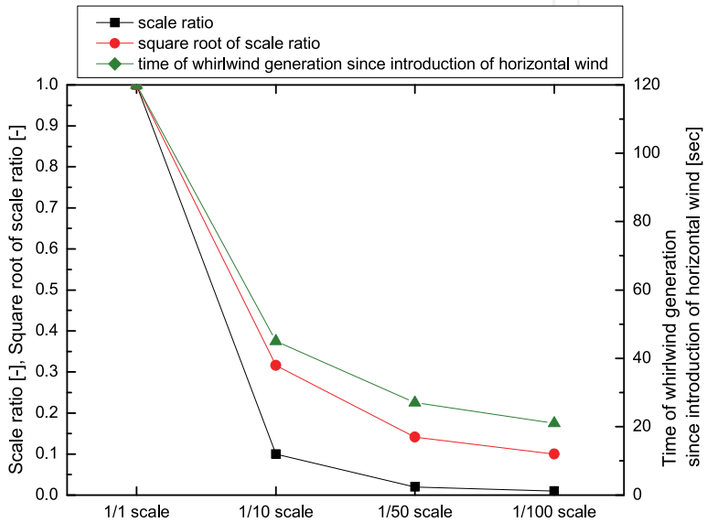

Fig. 17. Relation among scale ratio, square root of scale ratio, and time of whirlwind generation since introduction of horizontal wind in Model 1

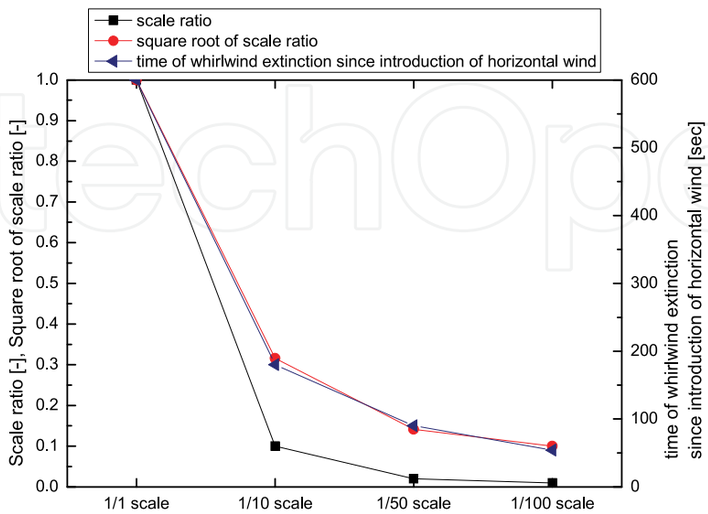

Fig. 18. Relation among scale ratio, square root of scale ratio, and time of whirlwind extinction since introduction of horizontal wind in Model 1

Fig. 19 shows relation among the scale ratio, the square root of scale ratio, and time of the strongest whirlwind generation since introduction of horizontal wind. The time of the strongest whirlwind generation is also more coincident with the square root of scale ratio rather than the scale ratio. Therefore, scale effect is recognized, in which time variation of whirlwind is coincident with the square root of scale ratio.

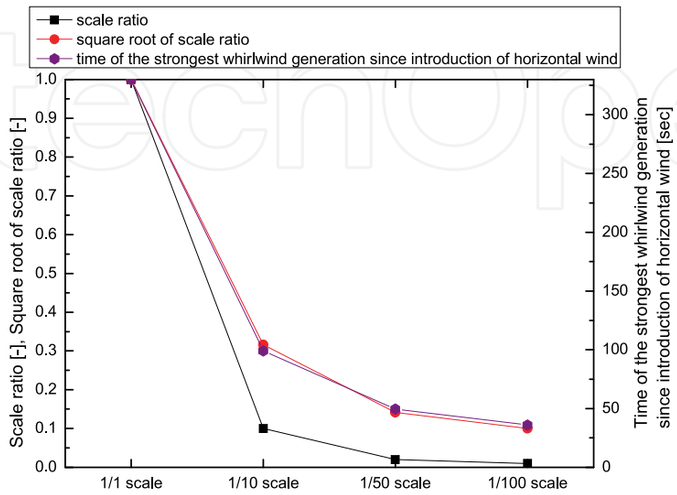

Fig. 19. Relation among scale ratio, square root of scale ratio, and time of the strongest whirlwind generation since introduction of horizontal wind in Model 1

5.2.2.3 Velocity of horizontal wind

Fig. 20 shows relation among the scale ratio, the square root of scale ratio, and appropriate velocity of horizontal wind to generate swirling flow. The appropriate velocity of horizontal wind to generate swirling flow is also more coincident with the square root of scale ratio rather than the scale ratio. Therefore, scale effect is recognized, in which velocity of horizontal wind is coincident with the square root of scale ratio.

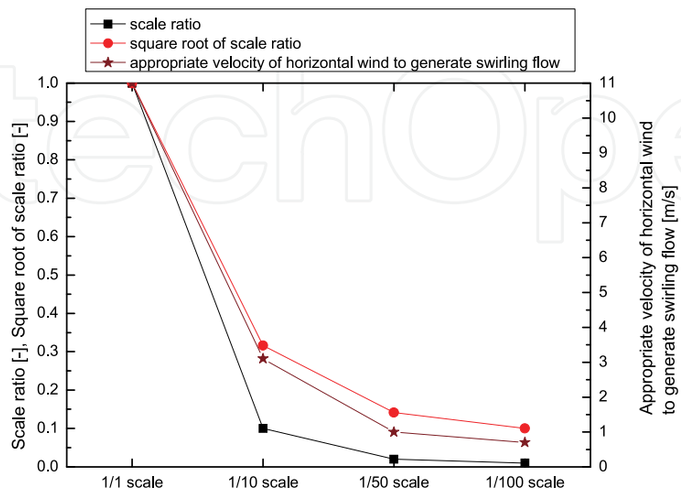

Fig. 20. Relation among scale ratio, square root of scale ratio, and appropriate velocity of horizontal wind to generate swirling flow in Model 1

5.2.3 Generation and extinction of swirling flow in Model 3

Fig. 21 shows samples of pressure field at the bottom surface and streamline distributions for the original scale simulation; (a) is at 2 minutes since the introduction of horizontal wind, (b) is at 4.5 minutes since the introduction of horizontal wind, and (c) is at 5.5 minutes since the introduction of horizontal wind. These streamlines are drawn from the bottom surface, and are colored by velocity magnitude.

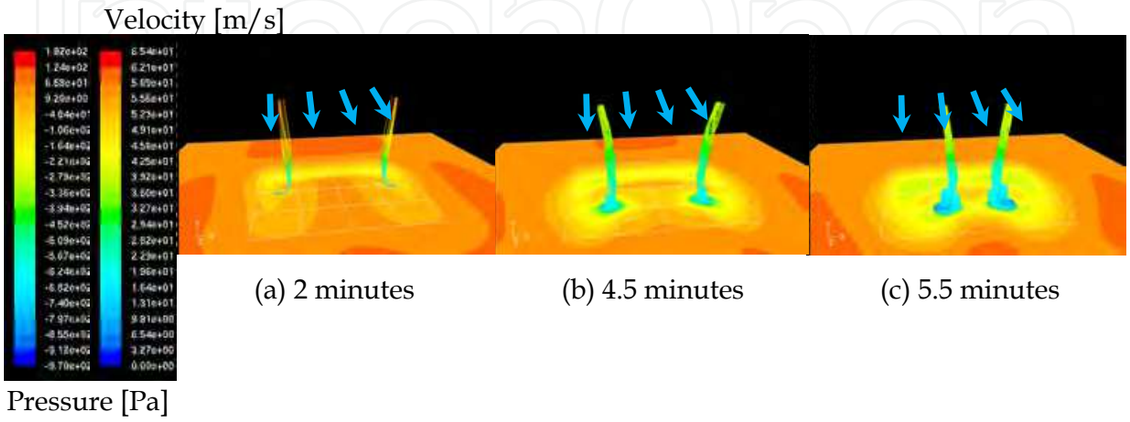

Fig. 21. Pressure field at the bottom surface and streamline distributions since the introduction of horizontal wind in Model 3

From Fig. 21 (a), two whirlwinds are generated and generation points of the whirlwind are located at the corners of "C" character. The whirlwinds are flown to the downstream, and are the strongest at this time (See Fig. 21 (b)). The maximum center pressure of the whirlwinds is lower than the atmospheric pressure by 970Pa. Then, the whirlwinds approach each other regardless of horizontal wind direction (See Fig. 21 (c)), and is remaining at 10 minutes since the introduction of horizontal wind.

Numerical calculation is performed not only for the case of the original size, but also for 1/10 scale, 1/50 scale and 1/100 scale. In the original size calculation, natural convection is developed in the domain after 5 minutes. The smaller the scale is, the shorter the time necessary to develop the natural convection is. The times necessary to develop the natural convection are 30 seconds for 1/10 scale model, 15 seconds for 1/50 scale model, and 9 seconds for 1/100 scale model. These values are smaller than those of L-character heat source. This is because the wider the area of heat source is, the more natural convection develops.

Introducing the appropriate velocity of horizontal wind to generate swirling flow in Model 1 as a velocity of horizontal wind, behavior of the whirlwind (movement and extinction) is observed for all the cases. While number of generated fire whirlwind is the same for all the cases, whirlwinds are not extinguished, and are still remained in the cases of the original size and 1/50 scale model. This is because the appropriate velocity of horizontal wind to generate swirling flow in Model 1 is larger or smaller compared with the appropriate velocity of horizontal wind to generate swirling flow in Model 3. Relation between configuration of heat source and horizontal wind velocity is one of the important roles to simulate generation and extinction of fire whirlwind. Despite of the difference in behavior of

the whirlwind, characteristic physical quantities of whirlwind are discussed by comparing with scale ratio and square root of scale ratio as well as in the case of Model 1.

5.2.3.1 Pressure of whirlwind

Fig. 22 shows relation among the scale ratio, the square root of scale ratio, and pressure at the bottom of natural convection after each period necessary to develop the natural convection.

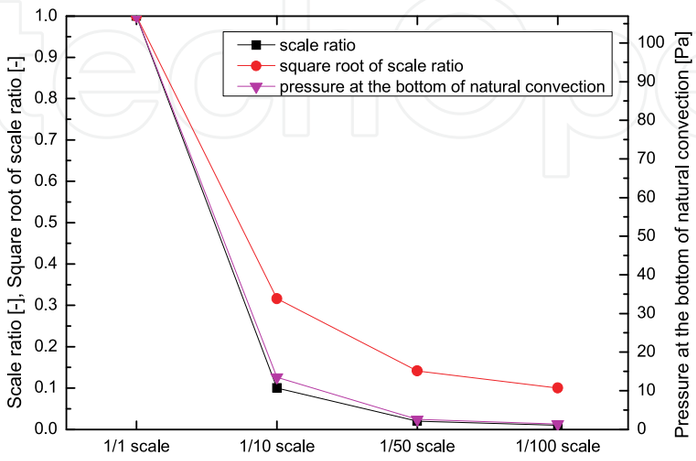

Fig. 22. Relation among scale ratio, square root of scale ratio, and pressure at the bottom of natural convection in Model 3

Taken the original size as a standard, the pressure at the bottom of natural convection is more coincident with the scale ratio rather than the square root of scale ratio.

Fig. 23 shows relation among the scale ratio, the square root of scale ratio, and the maximum center pressure of whirlwind, which is lower than the atmospheric pressure. The maximum center pressure of whirlwind is also more coincident with the scale ratio rather than the square root of scale ratio. Therefore, scale effect may be recognized, in which pressure of whirlwind is coincident with the scale ratio.

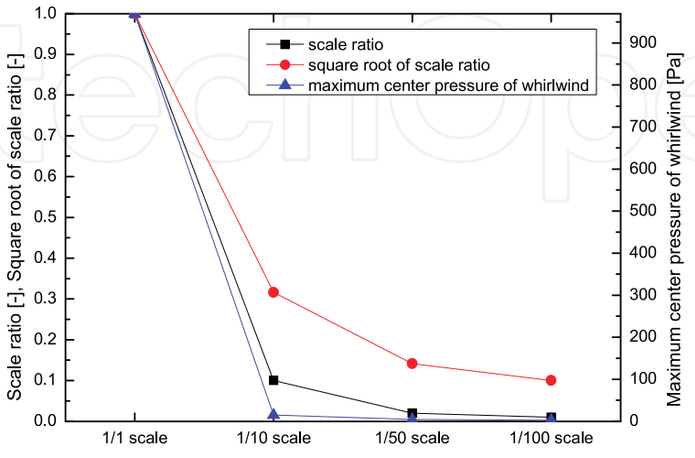

Fig. 23. Relation among scale ratio, square root of scale ratio, and maximum center pressure of whirlwind in Model 3

5.2.3.2 Time variation of whirlwind

Figs. 24 and 25 show relation among the scale ratio, the square root of scale ratio, and times of whirlwind generation and the strongest whirlwind generation since introduction of horizontal wind. Here is no discussion for time of whirlwind extinction, because whirlwinds are not extinguished, and are still remained in the cases of the original size and 1/50 scale model. The times of whirlwind generation and extinction since introduction of horizontal wind are more coincident with the square root of scale ratio rather than the scale ratio. Therefore, scale effect may be recognized, in which time variation of whirlwind is coincident with the square root of scale ratio.

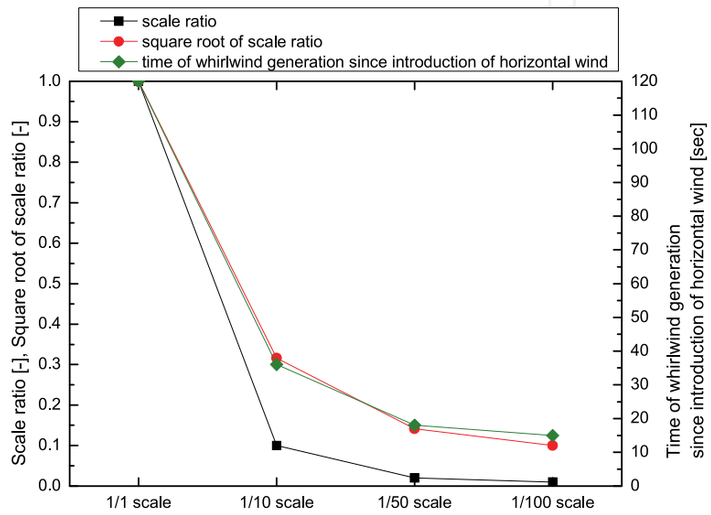

Fig. 24. Relation among scale ratio, square root of scale ratio, and time of whirlwind generation since introduction of horizontal wind in Model 3

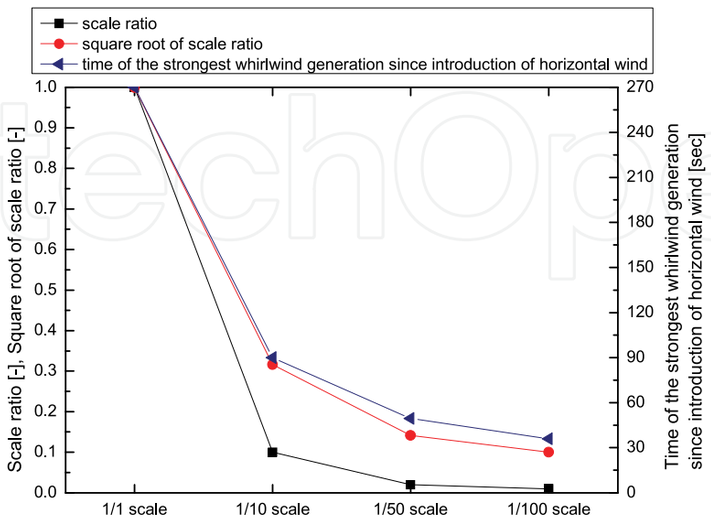

Fig. 25. Relation among scale ratio, square root of scale ratio, and time of whirlwind extinction since introduction of horizontal wind in Model 1

5.2.4 Summary

In this section, performing the numerical analysis of fire whirlwind with respect to scale effect, it is examined whether a relationship exists between a real phenomenon and the phenomenon in the reduction model with taking into account radiative heat transfer. It is clarified that the radiative heat exchange must be considered to precisely simulate the fire whirlwind, because the radiative heat transfer encourages the maximum upward velocity of natural convection and the appropriate velocity of horizontal wind due to the effective heat transfer. Scale effect is recognized in the L-character heat source model, in which pressure of whirlwind is coincident with the scale ratio, time variation of whirlwind and velocity of horizontal wind are coincident with the square root of scale ratio.

6. Conclusions

In this study, it is firstly aimed to get basic knowledge to elucidate outbreak mechanism of fire whirlwind and the property, by evaluating influence between a natural convection generated by the fire and the wind blowing to fire whirlwind on the ground utilizing numerical analysis.

- Interaction between the ascending current of air by natural convection and wind results in a fire whirlwind. The whirlwind sometimes moves and extinct. Generation points of the whirlwind are located at the tips and corner in the model of "L" character type. The points where the natural convective flow develops becomes origins of the fire whirlwind.
- Generation points of the whirlwind in the model of random type are located at the downstream heat source, and the number of the generated whirlwind is almost the same though the velocity of wind is varied.

It is secondly examined whether a relationship exists between a real phenomenon and the phenomenon in reduction models, performing the numerical analysis of a fire whirlwind with respect to scale effect.

- It is clarified that the radiative heat exchange must be considered to precisely simulate the fire whirlwind, because the radiative heat transfer encourages the maximum upward velocity of natural convection and the appropriate velocity of horizontal wind due to the effective heat transfer.
- Scale effect is recognized in the L-character heat source model, in which pressure of whirlwind is coincident with the scale ratio, time variation of whirlwind and velocity of horizontal wind are coincident with the square root of scale ratio.

7. References

Battaglia, F.; McGrattan, K. B.; Rehm, R. G. & Baum, H. R. (2000b). Simulating Fire Whirls, *Combustion Theory and Modelling*, Vol.4, No.3, pp.123-138

Battaglia, F.; Rehm, R. G. & Baum, H. R. (2000a). Fluid Mechanics of Fire Whirls: An Inviscid Model, *Physics of Fluids*, Vol.12, No.11, pp.2859-2867

Byram, G. M. & Martin, R. E. (1970). The Modeling of Fire Whirlwinds, *Forest Science*, Vol.16, No.4, pp.386-399

Chuah, K. H. & Kushida, G. (2007). The prediction of flame heights and flame shapes of small fire whirls, *Proceedings of the Combustion Institute*, Vol. 31, pp.2599–2606

Chuah, K. H.; Kuwana, K.; Saito, K. & Williams, F. A. (2011). Inclined fire whirls, *Proceedings of the Combuation Institute*, Vol.33, pp.2417-2424

Emmons, H. W. & Ying, S. J. (1967) The fire whirl, *Proceedings of the Combustion Institute*, Vol.11, pp. 475–488

Emori, R. I. & Saito, K. (1982). Model experiment of hazardous forest fire whirl, *Fire Technology*, Vol.18, No.4, pp.319-327

Fluent Inc./Fluent Asia Pacific (2006). *FLUENT 6.3 User's Guide*, Fluent Incorporated

Graham, H. E. (1955). Fire whirlwinds, *Bulletin American Meteorological Society*, Vol.36, pp. 99–103

Grishin, A. M. (2007). Effect of the Interaction between Fire Tornadoes on Their Propagation, *Doklady Physics*, Vol.52, No.10, pp. 521-522

Grishin, A. M.; Matvienko, O. V. & Rudi, Y. A. (2009). Mathematical Modeling of Gas Combustion in A Twisted Jet and of The Formation of A Fiery Whirlwind, *Journal of Engineering Physics and Thermophysics*, Vol.82, No.5, pp.906-913

Haines, D. A. & Updike, G. H. (1971). Fire Whirlwind Formation over Flat Terrain, *USDA Forest Service Research Paper*, NC-71

Hassan, M. I.; Kuwana, K.; Saito, K. & Wang, F. (2005). Flow Structure Of A Fixed-frame Type Firewhirl, *Proceedings of the Eighth International Symposium*, International Association for Fire Safety Science, Beijing, China, September 18-23, pp.951-962

Hayashi, Y.; Ohmiya, Y.; Iwami, T. & Saga, T. (2003). Experimental Study on Fire and Plume Properties Using BRI's Fire Wind Tunnel Facility, *International Journal for Fire Science and Technology*, Vol.22, pp.17-35

Hough, S. E. & Bilham, R. G. (2005). *After the Earth Quakes: Elastic Rebound on an Urban Planet*, Oxford University Press USA

Kuwana, K.; Sekimoto, K.; Saito, K. & Williams, F. A. (2007). Can We Predict the Occurrence of Extreme Fire Whirls?, *AIAA JOURNAL*, Vol.45, pp.16-19

Kuwana, K.; Sekimoto, K.; Saito, K. & Williams, F. A. (2008). Scaling fire whirls, *Fire Safety Journal*, Vol.43, No.4, pp.252-257

Liu, N. A. (2005). Experimental and Theoretical Investigation on Fire Interactions and the Induced Firewhirls in Square Fire Arrays, *Proceedings of Fifth NRIFD International Symposium on Forest Fires*, Tokyo, pp.293-301

Liu, N. A.; Liu, Q.; Deng, Z. H.; Satoh, K. & Zhu, J. P. (2007). Burn-out Time Data Analysis on Interaction Effects among Multiple Fires in Fire Arrays, *Proceedings of the Combustion Institute*, Vol.31, pp.2589-2597

Martin, R. E.; Pendleton, D. W. & Burgess, W. (1976). Effect of Fire Whirlwind Formation on Solid Fuel Burning Rates, *Fire Technology*, Vol.12, No.1, pp.33-40

Muraszew, A.; Fedele, J. B. & Kuby W.C. (1979). The fire whirl phenomenon, *Combustion and Flame*, Vol. 34, pp.29-45

Sakai, S. & Miyagi, N. (2010). Numerical Study of Fire Whirlwind Taking into Account Radiative Heat Transfer, *IOP Conference Series: Materials Science and Engineering*, Vol.10, 012031

Sakai, S. & Watanabe, Y. (2007). Numerical Study of Interaction between Natural Convection Flow and horizontal wind, *Proceedings of the FEDSM2007, 5th Joint*

ASME/JSME Fluids Engineering Conference, FEDSM2007-37212, San Diego, California, USA, July 30-August 2, 2007

Satoh, K. & Yang, K. T. (1996). Experimental Observations of Swirling Fires, *Proceedings of ASME Heat Transfer Division*, HTD-Vol.335, No.4, pp.393-400

Satoh, K. & Yang, K. T. (1997). Simulations of swirling fires controlled by channeled self-generated entrainment flows [A], *Fire Safety Sci.*, *Proceedings of the 5th International Symposium[C]*, pp.201-212

Siegel, R. & Howell, J. (2002). *Thermal Radiation Heat Transfer*, *4th Edition*, Taylor & Fransis

Snegirev, A. Y.; Marsden, J. A.; Francis, J. & Makhviladze, G. M. (2004). Numerical studies and experimental observations of whirling flames, *International Journal of Heat and Mass Transfer*, Vol.47, pp.2523–2539

Takewaki, I.; Murakami, S.; Fujita, K.; Yoshitomi, S. & Tsuji, M. (2011). The 2011 off the Pacific coast of Tohoku earthquake and response of high-rise buildings under long-period ground motions, *Soil Dynamics and Earthquake Engineering*, in press

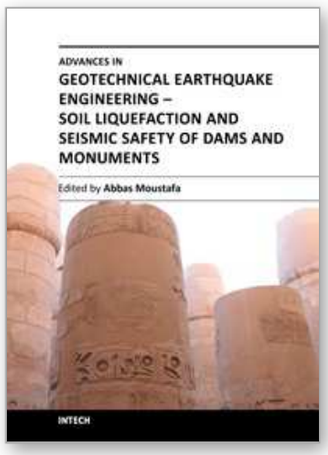

Advances in Geotechnical Earthquake Engineering - Soil Liquefaction and Seismic Safety of Dams and Monuments
Edited by Prof. Abbas Moustafa

ISBN 978-953-51-0025-6
Hard cover, 424 pages
Publisher InTech
Published online 10, February, 2012
Published in print edition February, 2012

This book sheds lights on recent advances in Geotechnical Earthquake Engineering with special emphasis on soil liquefaction, soil-structure interaction, seismic safety of dams and underground monuments, mitigation strategies against landslide and fire whirlwind resulting from earthquakes and vibration of a layered rotating plant and Bryan's effect. The book contains sixteen chapters covering several interesting research topics written by researchers and experts from several countries. The research reported in this book is useful to graduate students and researchers working in the fields of structural and earthquake engineering. The book will also be of considerable help to civil engineers working on construction and repair of engineering structures, such as buildings, roads, dams and monuments.

How to reference
In order to correctly reference this scholarly work, feel free to copy and paste the following:

Seigo Sakai (2012). Numerical Prediction of Fire Whirlwind Outbreak and Scale Effect of Whirlwind Behavior, Advances in Geotechnical Earthquake Engineering - Soil Liquefaction and Seismic Safety of Dams and Monuments, Prof. Abbas Moustafa (Ed.), ISBN: 978-953-51-0025-6, InTech, Available from: http://www.intechopen.com/books/advances-in-geotechnical-earthquake-engineering-soil-liquefaction-and-seismic-safety-of-dams-and-monuments/numerical-prediction-of-fire-whirlwind-outbreak-and-scale-effect-of-whirlwind-behavior

INTECH
open science | open minds

InTech Europe
University Campus STeP Ri
Slavka Krautzeka 83/A
51000 Rijeka, Croatia
Phone: +385 (51) 770 447
Fax: +385 (51) 686 166
www.intechopen.com

InTech China
Unit 405, Office Block, Hotel Equatorial Shanghai
No.65, Yan An Road (West), Shanghai, 200040, China
中国上海市延安西路65号上海国际贵都大饭店办公楼405单元
Phone: +86-21-62489820
Fax: +86-21-62489821

IntechOpen